THE JOURNAL OF PHYSICAL CHEMISTRY LETTERS
A JOURNAL OF THE AMERICAN CHEMICAL SOCIETY

pubs.acs.org/JPCL

Letter

Extracting Kinetics and Thermodynamics of Molecules without Heavy Atoms via Time-Resolved Solvent Scattering Signals

Key Young Oang, Sungjun Park, Jiwon Moon, Eunji Park, Hyun Kyung Lee, Tokushi Sato, Shunsuke Nozawa, Shin-ichi Adachi, Joonghan Kim, Jeongho Kim, Jeong-Hun Sohn,* and Hyotcherl Ihee*

Cite This: *J. Phys. Chem. Lett.* 2023, 14, 3103−3110

Read Online

ACCESS | Metrics & More | Article Recommendations | Supporting Information

ABSTRACT: Time-resolved X-ray liquidography (TRXL) has emerged as a powerful technique for studying the structural dynamics of small molecules and macromolecules in liquid solutions. However, TRXL has limited sensitivity for small molecules containing light atoms only, whose signal has lower contrast compared with the signal from solvent molecules. Here, we present an alternative approach to bypass this limitation by detecting the change in solvent temperature resulting from a photoinduced reaction. Specifically, we analyzed the heat dynamics of TRXL data obtained from *p*-hydroxyphenacyl diethyl phosphate (HPDP). This analysis enabled us to experimentally determine the number of intermediates and their respective enthalpy changes, which can be compared to theoretical enthalpies to identify the intermediates. This work demonstrates that TRXL can be used to uncover the kinetics and reaction pathways for small molecules without heavy atoms even if the scattering signal from the solute molecules is buried under the strong solvent scattering signal.

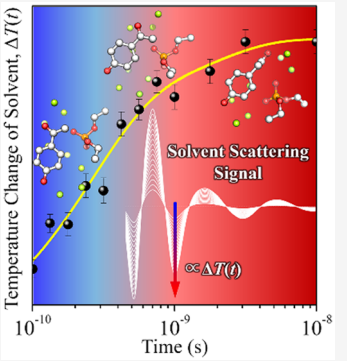

Time-resolved X-ray liquidography (TRXL), which is also known as time-resolved X-ray solution scattering, employs an optical pulse as the pump and the scattering of an X-ray pulse as the probe. This technique can be used to directly visualize the structural dynamics of various molecular systems in the liquid solution with the atomic-level sensitivity.[1−32] Thus far, the application of TRXL has been limited to the solute molecules containing heavy atoms because the high-intensity scattering of the heavy atoms prevents the scattering signal of the solutes from being obscured by large background scattering from solvent molecules in a dilute solution. For solute molecules lacking heavy atoms, a strategy of chemically attaching heavy atoms to the solute molecule has been used to increase the scattering contributions of solutes,[1,2,5,6,9,14,22,29,31] but such chemical modification may lead to a change in reaction dynamics. Regarding the limited applicability of current TRXL, a recent study proposed that it is in principle possible to directly visualize the motions of solute molecules without heavy atoms once next-generation X-ray sources such as LCLS-II HE become available.[32]

As a step toward this goal, here we present an alternative way of extending the applicability of TRXL to a broader range of molecular systems by using the scattering signal of solvent molecules. Specifically, we take advantage of the fact that the heat exchange between solute and solvent molecules during a reaction induces the change in the solvent temperature and accordingly the solvent scattering. In principle, the TRXL signal of a solution sample comprises three principal components: solute-only term, solute−solvent cross term, and solvent-only term.[3,10,12,27] Among these components, the solvent-only term is highly sensitive to the variation of temperature, T, and density, ρ, of the solvent. These thermodynamic parameters change sensitively with the heat exchange between light-absorbing solute molecules and their surrounding solvent molecules with the progress of a reaction, as illustrated in Figure 1. As a result, the scattering response of solvent also changes over time with the changes of temperature and density, giving rise to the time-resolved solvent heating response manifested as $q(\partial S/\partial T)_\rho \Delta T(t)$ at early time delays (on the time scale of tens of picoseconds) and $q(\partial S/\partial \rho)_T \Delta\rho(t)$ at late time delays (on the time scale of hundreds of nanoseconds).[3] Especially, at the early time delays after photoexcitation, the solvent scattering intensity changes linearly with the temperature change of the solvent. Thus, the solvent response of TRXL can be used as an ultrafast thermometer and/or densimeter with high sensitivity. This strategy of monitoring the heat exchange can be applied even to the solution-phase reactions of molecules without any heavy atom, as long as the heat exchange with the surrounding

Received: January 5, 2023
Accepted: March 20, 2023

https://doi.org/10.1021/acs.jpclett.3c00041
J. Phys. Chem. Lett. 2023, 14, 3103−3110

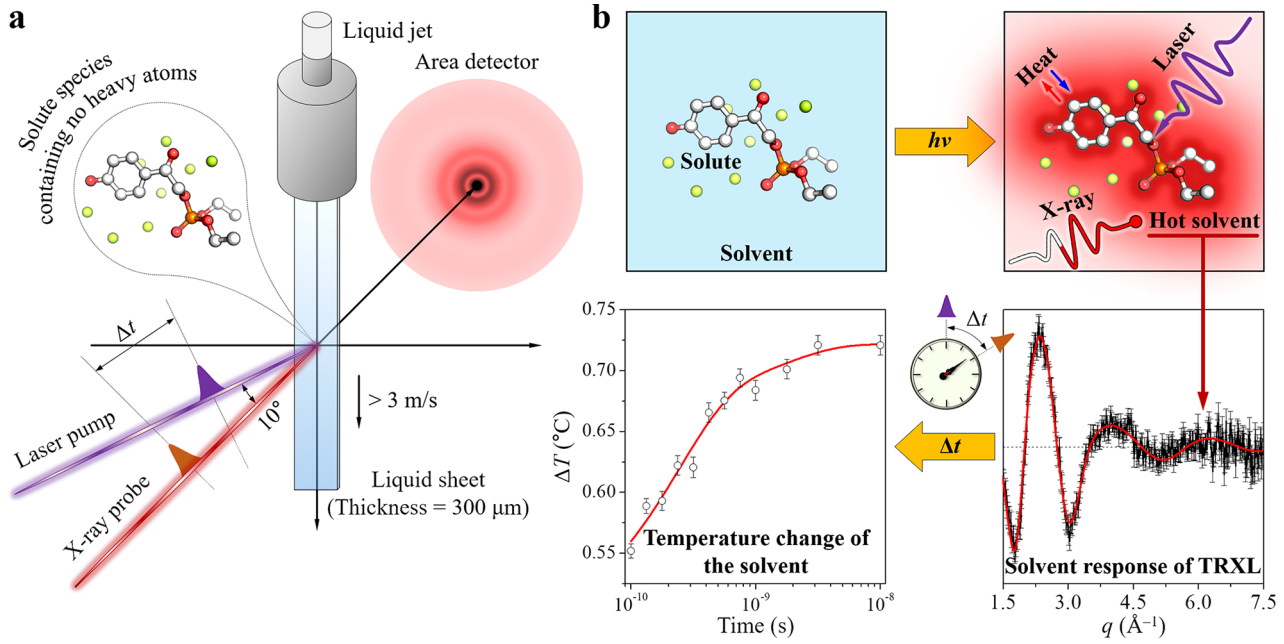

Figure 1. Scheme of a TRXL experiment at an X-ray facility and the workflow of data analysis. (a) Solute molecules in a solution are excited by a laser pulse. Subsequently, a picosecond X-ray pulse incident with a time delay, Δt, probes the changes in the solvent scattering with the progress of the photoinduced reaction of solute molecules. In this experiment, the X-ray beam propagated along the x-axis and the sample was flown along the z-axis. The laser beam was overlapped with the X-ray beam at the focal point at a crossing angle of 10°. (b) Probing of the temperature change of the solvent as a means of investigating the reaction dynamics of solute molecules. Most importantly, the linear dependence of the solvent scattering signal on the temperature change of the solvent allows us to estimate the absolute amount of heat exchange between the solute and solvent molecules.

solvent molecules occurs during the reaction. In other words, the solvent heating response can serve as an excellent tool for monitoring the dynamics of a photochemical reaction, regardless of the presence of heavy atoms in the molecular systems of interest.

In this work, by analyzing the solvent-only term of the TRXL data, we address the kinetic components and reaction mechanism of a small molecule without heavy atoms. For this purpose, we chose the photoinduced reaction of *p*-hydroxyphenacyl diethyl phosphate (HPDP), which consists of the *p*-hydroxyphenacyl (*p*HP) cage and the leaving group of diethyl phosphate. The *p*HP group is an efficient phototriggerable cage that can be used for the liberation of various chemicals and biological stimulants.[33−54] In particular, the *p*HP group has been envisioned as a phototrigger for real-time monitoring of physiological responses in nonphotoactive biological systems such as proteins and DNAs. In an aqueous environment, the photolysis of the *p*HP group induces the photo-Favorskii rearrangement (also known as the photosolvolytic rearrangement), which converts the *p*HP cage into *p*-hydroxyphenylacetic acid (HPAA).[33−54] For the photo-Favorskii rearrangement, several plausible reaction mechanisms were proposed based on time-resolved spectroscopic and theoretical studies,[40,42,43,46,50] but its reaction mechanism and reaction intermediates are still in debate due to discrepancies between those studies. For example, as summarized in Figure S1 and Table S1 in the Supporting Information, there have been controversies regarding the identities of reaction intermediates among solvated triplet species of contact ion pair character (^{3}CIP), allyloxy−phenoxy triplet biradical (^{3}AP), and spirodienedione (^{1}SK).[40,42,43,46,50] We extract reaction-induced enthalpy changes ΔH_{exp} of HPDP from the TRXL data and offer a plausible mechanism by comparing ΔH_{exp} with the theoretical ones, ΔH_{DFT}, calculated for the candidate intermediate species of the reaction.

In Figure 2, difference TRXL curves, $q\Delta S(q,t)$, measured for a solution sample of HPDP (Figure 2a) are shown together

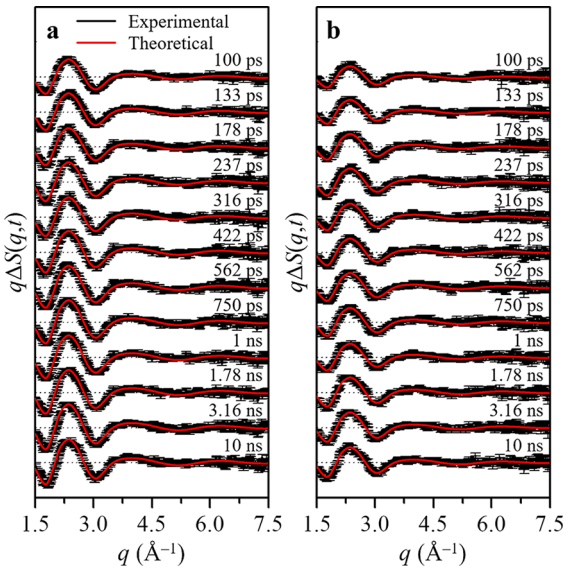

Figure 2. Time-resolved difference X-ray solution scattering curves (black), $q\Delta S(q,t)$, measured from the TRXL experiment and theoretical scattering curves (red) for a solution sample of (a) HPDP and (b) $FeCl_3$ in H_2O/MeCN cosolvent. The time delay after photoexcitation is indicated above each curve. Theoretical scattering curves were generated by multiplying $q(\partial S/\partial T)_\rho$ calculated from the MD simulation with the time-dependent temperature of the bulk cosolvent obtained from the TRXL measurement.

https://doi.org/10.1021/acs.jpclett.3c00041
J. Phys. Chem. Lett. 2023, 14, 3103−3110

with $q\Delta S(q,t)$ measured for a solution sample of $FeCl_3$ (Figure 2b) in H_2O/MeCN (2:1, v/v). The latter measurement was performed as a control experiment for obtaining only the contribution of the heating of H_2O/MeCN, without any contribution of structural change of the solutes (see the Supporting Information for details). Since HPDP and $FeCl_3$, which were used as solutes in this work, do not contain any heavy-atom constituent (in the case of HPDP) or do not involve any noticeable structural change (in the case of $FeCl_3$),[21,23,32] we expect that $q\Delta S(q,t)$ from both samples would be dominated by the solvent-only signals (see Figure S3). Especially, because we measured the TRXL data in the time range of 100 ps to 10 ns, whose upper limit is much earlier than the onset time for the density change of solvent (~100 ns in this work),[3] $q\Delta S(q,t)$ would be described simply by $q(\partial S/\partial T)_\rho$ multiplied by $\Delta T(t)$. The $q(\partial S/\partial T)_\rho$ term is the specific change of scattering pattern characteristic of a solvent, and $\Delta T(t)$ is a quantity that varies in proportion to the enthalpy change (ΔH) characteristic of a photochemical reaction.

To examine our prediction described above, we first extracted a scattering pattern common to both solution samples (presumably $q(\partial S/\partial T)_\rho$ of the H_2O/MeCN) by performing singular value decomposition (SVD) analysis[28] simultaneously for the TRXL data of HPDP and those of $FeCl_3$. SVD decomposes the original data into time-invariant features (left singular vectors, LSVs), their relative contributions (singular values), and their time profiles (right singular vectors, RSVs). From the SVD analysis in the q range of 1.5−7.5 $Å^{-1}$ and the time range of 100 ps to 10 ns, only a single LSV (which is common for the TRXL data of HPDP and those of $FeCl_3$) and its corresponding RSV (which is each for the data of HPDP and those of $FeCl_3$) showed significant contributions, whereas the rest account for noises as shown in Figure S4. To understand the origin of the sole significant LSV, we performed the MD simulation for the neat H_2O/MeCN using the MOLDY program,[55] as shown in Figure S4b. Two thermodynamic conditions of the solvent (C_1: T_1 = 300 K, ρ_1 = 929 kg/m^3; C_2: T_2 = 330 K, ρ_2 = 929 kg/m^3) were considered in the MD simulation. From the simulation, $q(\partial S/\partial T)_\rho$ was obtained from the difference between the scattering intensity of the solvent at C_2 and the one at C_1 divided by the temperature change ($\Delta T = T_2 - T_1$). It can be seen in Figure S4a that $q(\partial S/\partial T)_\rho$ calculated from the MD simulation is in excellent agreement in its shape with the principal LSV obtained from the SVD analysis, indicating that the principal LSV corresponds to $q(\partial S/\partial T)_\rho$ of the H_2O/MeCN and furthermore confirming our prediction that $q\Delta S(q,t)$ would be described simply by $q(\partial S/\partial T)_\rho$ multiplied by $\Delta T(t)$.

In general, from the TRXL data measured for a solution sample, one may extract multiple principal LSVs and their corresponding principal RSVs.[21,24,28,32] The LSVs are time-independent scattering patterns and, when combined together, give the structural information on solute species involved in a photoinduced reaction, that is, reactant, intermediate, and product species. The RSVs are temporal profiles of the amplitudes of the LSVs and contain information on the population kinetics of the solute species. In many cases, for the TRXL data measured for solution samples of heavy-atom-containing solutes, the SVD analysis gives the information on how many structurally distinguishable transient solute species are involved in the dynamic processes of interest and how fast the population of each solute species changes after photoexcitation. This is possible because the large scattering of the heavy atoms allows for achieving a signal-to-noise ratio high enough for distinguishing the solute-related signals (that is, solute-only and solute−solvent cross terms) against the solvent-only signal, which generally dominates the solution scattering signal.[3,10,12,27] In this work, however, the only principal LSV identified commonly for both HPDP and $FeCl_3$ solution samples corresponds to the solvent heating response induced by the temperature change of solvent at a constant density, $q(\partial S/\partial T)_\rho$, while its corresponding principal RSV identified separately for HPDP and $FeCl_3$ solution samples contains the information on the dynamics and the absolute amount of heat transfer between the solutes and the solvent for the cases of HPDP and $FeCl_3$, respectively.

Figure 3a shows the difference TRXL curve of HPDP measured at 100 ps after photoexcitation, $q\Delta S(q,t$ = 100 ps), which is well fit by $q(\partial S/\partial T)_\rho$ (shown in Figure S4b) multiplied by the temperature change (approximately +0.55 °C) at 100 ps after photoexcitation, $\Delta T(t$ = 100 ps). Before fitting $q\Delta S(q,t$ = 100 ps) to find $\Delta T(t$ = 100 ps), we first appropriately scaled the experimental scattering curve of HPDP by using the absolute scaling factor, $\alpha\beta$, described in the Supporting Information. In the same way, as in Figure 3a, we determined $\Delta T(t)$ at all time delays from the experimental $q\Delta S(q,t)$ from 100 ps to 10 ns (see Figure 3b). The obtained $\Delta T(t)$ is the same as the first RSV in its shape (see Figure S4c,d). For $FeCl_3$, $\Delta T(t)$ can be fit well with a single exponential with a relaxation time of 70 ± 30 ps, indicating that $FeCl_3$ molecules release heat into the surrounding solvent only by vibrational cooling.[21,23,32] The relaxation times associated with the photochemical reaction of HPDP were determined by fitting $\Delta T(t)$ of HPDP using a sum of two exponentials. From the fitting, we obtained the relaxation times of 230 ± 20 ps and 1.7 ± 0.6 ns for HPDP as shown in Figure

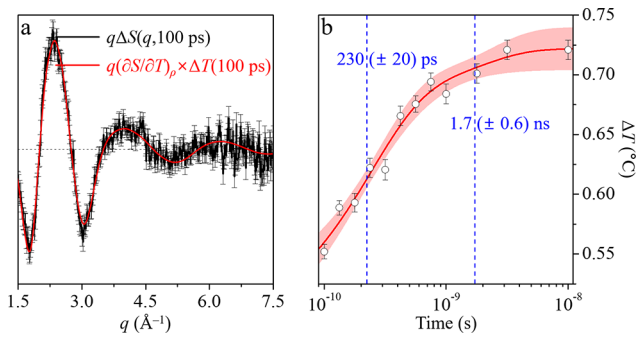

Figure 3. Temperature changes of the bulk cosolvent due to the photochemical-reaction-induced energy exchange between the solute (HPDP) and the cosolvent (H_2O/MeCN mixture) molecules. (a) TRXL data of HPDP measured at 100 ps (black) are well fitted by the scattering intensity change from bulk cosolvent arising from the temperature change at a constant density, $(\partial S/\partial T)_\rho$, multiplied by the temperature change at 100 ps (red). The experimental errors are indicated by vertical lines. (b) Time-dependent temperature changes of the bulk cosolvent due to the photochemical-reaction-induced energy exchange between the solute (HPDP) and the cosolvent (H_2O/MeCN mixture) molecules are shown (black open circles). The experimental errors are indicated by vertical lines. Red curve was obtained by performing the fitting analysis of hydrodynamics. The shaded area indicates a 95% confidence interval, which represents a range of values within which the true value is expected to fall with 95% probability.

https://doi.org/10.1021/acs.jpclett.3c00041
J. Phys. Chem. Lett. 2023, 14, 3103−3110

S5. To verify the validity of using two exponentials to fit $\Delta T(t)$ of HPDP, we tested fits using fewer or more exponentials. With a single exponential, the fit quality significantly deteriorates. Using three exponentials does not result in a noticeable improvement in the fit quality, supporting the use of two exponentials for fitting the $\Delta T(t)$ of HPDP (see Figure S6a). The obtained relaxation times were used in the fitting analysis of hydrodynamics based on a kinetic model, the details of which will be described later.

To identify the intermediate species of the photochemical reaction of HPDP, we extracted the enthalpy changes, ΔH_{exp}, of the intermediate species by following the temperature change of the solvent. In the fitting analysis of hydrodynamics,[2] by minimizing the discrepancy quantified by the χ^2 value between the experimentally obtained temperature changes (black open circles in Figure 3b) and the theoretically calculated ones (red solid curve in Figure 3b), we optimized ΔH_{exp} of the intermediate species involved in the reaction. In choosing the optimum kinetic model in our previous TRXL studies,[15,20,25,28] the results of SVD analysis, that is the number of distinct solute species and the number of kinetic components, often led us to consider more complex kinetic models than a simple sequential kinetic model. For example, those complex kinetic models include biphasic kinetics, backward reaction pathways such as geminate recombination, and bimolecular reaction pathways. Unlike those cases, the SVD results in this work only tell us the number of kinetic components and do not provide information on the number of distinct solute species. Two apparent relaxation times pose two possible assignments: (i) 230 ps corresponds to vibrational cooling of HPDP, and only a single relaxation time, 1.7 ns, accounts for a process related to the photo-Favorskii rearrangement, and (ii) both 230 ps and 1.7 ns account for the processes related to the photo-Favorskii rearrangement. Based on the facts that (1) the time scale of vibrational cooling in liquid solution is typically faster than the temporal resolution of our TRXL measurement (100 ps)[2,3,8,10,12−14,17,18,27,31] and (2) the relaxation time of 230 ps obtained in this work follows well the dependence of the decay dynamics of ^{3}CIP on the water fraction in the cosolvent reported in previous studies,[40,43,46,50] we assigned the two relaxation times (230 ps and 1.7 ns) to the photo-Favorskii rearrangement. In addition, by following the previously proposed kinetic frameworks shown in Figure S1, we considered a simple sequential kinetic model containing three species (A, B, and C) and two relaxation times (230 ps for A → B and 1.7 ns for B → C) shown in Figure 4. The assignment suggests that the HPDP data are minimally affected by vibrational cooling and does not reveal the relaxation time for this process. However, prior to performing the hydrodynamic fitting analysis, we were uncertain about the extent to which vibrational cooling contributed to the HPDP data. As a result, we introduced the fitting parameter (f_{vib}) to account for the relative contribution of vibrational cooling to the data and to consider the fast recovery of the ground state of HPDP via vibrational cooling. In the absence of any contribution of vibrational cooling, f_{vib} would converge to zero in the fitting results. In addition, because the HPDP data are not strongly sensitive to the relaxation time for vibrational cooling, we simply assumed that the relaxation time for vibrational cooling of HPDP is the same as that of $FeCl_3$ (70 ps) in order to determine the relative contribution of vibrational cooling (f_{vib}) in the case of HPDP. From the fitting analysis of hydrodynamics, we determined that 36.5 ± 1.3% of the photoexcited HPDP molecules undergo the photo-Favorskii rearrangement, which is consistent with previous studies (33−40%),[33,40,42,43,46,50] and 1.8 ± 0.2% of the photoexcited molecules relax to the ground state via vibrational cooling (see the Supporting Information for details). The errors here account for only random errors, not systematic errors. Judging from the quantum yields of photo-Favorskii rearrangement and vibrational cooling we obtained in this work, the remainder (61.7 ± 1.5%) is likely to rapidly relax to the ground state without heat release into the surrounding solvent via fluorescence emission from the initially populated singlet excited states.[38] ΔH_{exp} of the three intermediate species were determined to be 249 ± 10 kJ/mol for A, 178 ± 14 kJ/mol for B, and 160 ± 13 kJ/mol for C relative to the enthalpy of the HPDP parent molecule in the ground state. In addition, here we note that even if a much faster relaxation time, for example, 10 ps, is used instead of 70 ps as the relaxation time for vibrational cooling in the fitting analysis of hydrodynamics, there is no significant difference in the relative contribution of vibrational cooling (f_{vib}) in the case of HPDP.

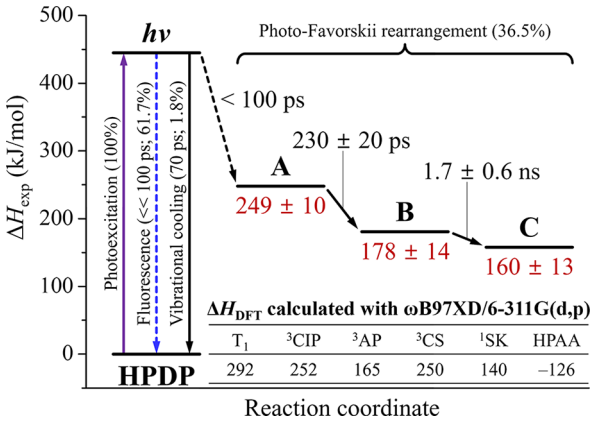

Figure 4. Mechanism of photoinduced reaction of HPDP in H_2O/MeCN and enthalpy levels of the chemical species involved in the reaction. The enthalpy levels (in kJ/mol) shown in the diagram are relative to the enthalpy of the HPDP parent molecule in the ground state. The relaxation times (70 ps for vibrational cooling, 230 ps for A → B, and 1.7 ns for B → C) and fractions (36.5% for photo-Favorskii rearrangement, 1.8% for vibrational cooling, and 61.7% for fluorescence emission) as well as enthalpies (249 kJ/mol for A, 178 kJ/mol for B, and 160 kJ/mol for C) were obtained from the TRXL data. The enthalpy values from DFT calculations with ωB97XD/6-311G(d,p) are also listed in the inset table for comparison.

The ΔH_{exp} values of the three intermediate species determined via analyzing the TRXL data are the key observables crucial for determining the reaction mechanisms and pathways via comparison with the calculated enthalpy changes. For this purpose, by performing DFT calculations,[56] we calculated the enthalpy changes, ΔH_{DFT}, relative to the enthalpy of the HPDP parent molecule in the ground state, of major candidate species that were proposed in previous studies (see Figure S1).[40,42,43,46,50] Specifically, the chemical species considered in the DFT calculations include (i) triplet excited state (T_1), (ii) solvated triplet species of contact ion pair character (^{3}CIP), (iii) allyloxy−phenoxy triplet biradical (^{3}AP), (iv) triplet cation species (^{3}CS), (v) spirodienedione (^{1}SK), and (vi) *p*-hydroxyphenylacetic acid (HPAA). We performed several DFT calculations, including B3LYP, CAM-B3LYP, M06-2X, MN12-SX, and MN15, for HPDP with eight

https://doi.org/10.1021/acs.jpclett.3c00041
J. Phys. Chem. Lett. 2023, 14, 3103−3110

or thirteen explicit water molecules. The calculated results are summarized in Table S2 in the Supporting Information. It should be noted that the calculated ΔH's can significantly depend on the method, level, and model of calculations. For example, different levels of calculations yielded different sets of ΔH_{DFT} values. The DFT calculations with ωB97XD/6-311G(d,p) gave ΔH_{DFT} of 292 kJ/mol, 252 kJ/mol, 165 kJ/mol, 250 kJ/mol, 140 kJ/mol, and −126 kJ/mol for T_1, ^{3}CIP, ^{3}AP, ^{3}CS, ^{1}SK, and HPAA, respectively. In the following, we attempt to assign the three species visible in the TRXL data to plausible species, based on these ΔH_{DFT} values.

The comparison of ΔH_{DFT}'s of the candidate species, T_1, ^{3}CIP, ^{3}AP, ^{3}CS, and ^{1}SK, with ΔH_{exp} of the first two species supports the assignment of A to ^{3}CIP and B to ^{3}AP. Specifically, ^{3}CIP is formed within 100 ps, which is the time resolution of the TRXL measurement, and subsequently transforms to ^{3}AP with a relaxation time of 230 ps (see Figure 4). This assignment regarding the formation and decay dynamics of ^{3}CIP is consistent with the previous studies using TA, TRIR, and TR^3 spectroscopy.[40,43,46,50] Especially, the rate of ^{3}CIP decay obtained in this work (1/230 ps^{-1}) for the solution sample of HPDP in H_2O/MeCN (2:1, v/v) is faster than the rate obtained previously[40] (1/350 ps^{-1}) for the same sample in less aqueous H_2O/MeCN (1:1, v/v), confirming the dependence of the decay dynamics of ^{3}CIP on the water fraction in the cosolvent as reported in the previous studies.[40,43,46,50] In addition, we can exclude the P2 pathway of the proposed mechanism 3 (see Figure S1), where ^{3}CS is formed from ^{3}CIP and then transforms to HPAAH$^+$ and HPAA sequentially because ΔH_{DFT} of ^{3}CS is too high (250 kJ/mol) compared with ΔH_{exp} of the second species (178 kJ/mol) determined from the TRXL measurement.

We can assign the third species (C) identified from the TRXL measurement to HPAA because its formation time, 1.7 ns, is the closest to that of HPAA determined from the previous time-resolved spectroscopic studies (see Figure 4).[40,43,50] Still, the 1.7 ns relaxation time assigned to the formation of HPAA is larger than the values (470 and 600 ps) reported in previous time-resolved spectroscopic studies.[40,43,50] Thus, we checked the fitting quality of the TRXL data by varying two relaxation times (τ_1 for A → B and τ_2 for B → C) to demonstrate their statistical significance and visually illustrate the confidence level of two relaxation times. As can be seen in Figure S6b, we obtained the best fitting quality when we fit the data with 230 ps and 1.7 ns. The discrepancy between previously reported values for τ_2 (470 and 600 ps) and the value obtained in this work (1.7 ns) suggests that the relaxation time obtained from TRXL may be slower than that obtained from transient absorption spectroscopy for the former method that is expected to be more responsive to the motion of both solute and solvent. It will be possible to determine the value of τ_2 more unambiguously if our TRXL data have more time points, especially on the nanosecond time scale. In Table S1, we compared the chemical species and the associated relaxation times determined in this work with the results of previous studies.

It is noteworthy that ΔH_{DFT} of HPAA (−126 kJ/mol) deviates significantly from ΔH_{exp} (160 kJ/mol) of the third species determined from the TRXL measurement, indicating improper description of the hydrogen-bonding network (HBN) of water molecules around ^{1}SK and HPAA molecules in the DFT calculations.[57,58] In our DFT calculations, we considered the solute−solvent interaction by explicitly solvating a solute molecule by only eight water molecules. The good agreement between ΔH_{DFT}'s of ^{3}CIP and ^{3}AP with ΔH_{exp} of the first two species suggests that eight explicit water molecules are sufficient to account for the solvation effect in the reaction steps from HPDP to ^{1}SK where no water molecule directly participates in. In contrast, for the reaction from ^{1}SK to HPAA, one water molecule directly reacts with ^{1}SK, resulting in the breaking and formation of covalent bonds (solvolytic reaction),[42,46] and thus the HBN needs to be properly described to calculate their ΔH_{DFT}'s accurately. Such a task to describe a realistic HBN would require solvation shells consisting of thousands of water molecules, and therefore it is currently not feasible in the DFT calculations (see the Supporting Information for details). Nevertheless, if the HBN can be described more realistically in the DFT calculations, we expect that ΔH_{DFT} of HPAA will be lower than but similar to that of ^{1}SK (140 kJ/mol). With this scenario, ^{1}SK must convert to HPAA rapidly as reported previously (see Figure 4).[43,50]

In summary, we investigated the solution-phase reaction dynamics of HPDP without heavy atom by probing the change of TRXL signal induced by the change in solvent temperature. We showed that TRXL can provide information on the kinetics of intermediates and their energy values, which can be combined with other methods like DFT calculation to identify intermediates. This highlights the potential utility of the approach. This approach, however, certainly has some limitations. First of all, the calculated enthalpies, ΔH_{DFT}, may depend on the DFT methods and the employed solvated environment of HPDP. Table S2 shows that except for B3LYP and CAM-B3LYP, all DFT methods yield similar ΔH_{DFT} values. However, the results depend significantly on the number of explicit water molecules used. For instance, in all DFT calculations with 13 explicit water molecules, the ^{3}CIP state converged to the ^{3}AP state. These findings indicate that the ΔH_{DFT} values can vary significantly with the number of explicit water molecules. In addition, if multiple candidate species of similar enthalpies or multiple competing pathways occurring at similar rates are involved in the reaction, it would be challenging to distinguish those species and reaction pathways. Despite these limitations, the TRXL approach of probing the heat transfer can still be a valuable tool for studying the reaction dynamics, particularly when combined with potential enhancements. First, by using solvents containing much heavier atoms than the atoms in solutes, the amount of structural information on the solute molecules can be increased (that is, the amplification of the solute−solvent cross term of the TRXL signal).[8] Second, one may be able to distinguish multiple competing pathways of similar rates by making use of solvent kinetic isotope effect. Third, next-generation X-ray sources such as LCLS-II HE should make it possible not only to investigate the energetics of solute molecules without heavy atoms but also to directly visualize their motions.[32] This approach of keeping track of the kinetics and thermodynamics for the solution-phase photochemical reactions, regardless of the presence of heavy atoms or the involvement of the spectroscopically transparent species in a reaction, is expected to stimulate further studies on various photochemical reactions and associated heat-exchange processes in solution.

https://doi.org/10.1021/acs.jpclett.3c00041
J. Phys. Chem. Lett. 2023, 14, 3103−3110

■ ASSOCIATED CONTENT

Supporting Information

The Supporting Information is available free of charge at https://pubs.acs.org/doi/10.1021/acs.jpclett.3c00041.

Sample preparation, TRXL data collection, SVD analysis, MD simulations, solvent response, absolute scaling factor and temperature change of the solvent, fitting analysis of hydrodynamics, a summary of previous studies of the photoinduced reaction dynamics of HPDP in H_2O/MeCN, quantum yield of the photo-Favorskii rearrangement, DFT calculations, and related figures and materials (PDF)

Transparent Peer Review report available (PDF)

■ AUTHOR INFORMATION

Corresponding Authors

Jeong-Hun Sohn − *Department of Chemistry, College of Natural Sciences, Chungnam National University, Daejeon 34134, Republic of Korea;* orcid.org/0000-0001-8800-7941; Email: sohnjh@cnu.ac.kr

Hyotcherl Ihee − *Department of Chemistry and KI for BioCentury, Korea Advanced Institute of Science and Technology (KAIST), Daejeon 34141, Republic of Korea; Center for Advanced Reaction Dynamics, Institute for Basic Science (IBS), Daejeon 34141, Republic of Korea;* orcid.org/0000-0003-0397-5965; Email: hyotcherl.ihee@kaist.ac.kr

Authors

Key Young Oang − *Radiation Center for Ultrafast Science, Korea Atomic Energy Research Institute (KAERI), Daejeon 34057, Republic of Korea*

Sungjun Park − *Department of Chemistry and KI for BioCentury, Korea Advanced Institute of Science and Technology (KAIST), Daejeon 34141, Republic of Korea; Center for Advanced Reaction Dynamics, Institute for Basic Science (IBS), Daejeon 34141, Republic of Korea*

Jiwon Moon − *Department of Chemistry, The Catholic University of Korea, Bucheon 14662, Republic of Korea*

Eunji Park − *Department of Chemistry, The Catholic University of Korea, Bucheon 14662, Republic of Korea;* orcid.org/0000-0003-1214-8822

Hyun Kyung Lee − *Department of Chemistry, College of Natural Sciences, Chungnam National University, Daejeon 34134, Republic of Korea*

Tokushi Sato − *European XFEL, 22869 Schenefeld, Germany*

Shunsuke Nozawa − *Institute of Materials Structure Science, High Energy Accelerator Research Organization, Tsukuba, Ibaraki 305-0801, Japan;* orcid.org/0000-0003-4977-6849

Shin-ichi Adachi − *Institute of Materials Structure Science, High Energy Accelerator Research Organization, Tsukuba, Ibaraki 305-0801, Japan; Department of Materials Structure Science, School of High Energy Accelerator Science, The Graduate University for Advanced Studies, Tsukuba, Ibaraki 305-0801, Japan;* orcid.org/0000-0002-3676-1165

Joonghan Kim − *Department of Chemistry, The Catholic University of Korea, Bucheon 14662, Republic of Korea;* orcid.org/0000-0002-7783-0200

Jeongho Kim − *Department of Chemistry, Inha University, Incheon 22212, Republic of Korea;* orcid.org/0000-0003-4085-293X

Complete contact information is available at: https://pubs.acs.org/10.1021/acs.jpclett.3c00041

Author Contributions

H.I. supervised the project. J.-H.S. and H.I. designed the experiment. K.Y.O., S.P., H.K.L., T.S., S.N., S.-i.A., Je.K., J.-H.S., and H.I. performed the experiments. K.Y.O. and S.P. analyzed the data. J.M., E.P., and Jo.K. performed quantum chemical calculations. K.Y.O., Jo.K., Je.K., J.-H.S., and H.I. wrote the manuscript with contributions from all authors.

Notes

The authors declare no competing financial interest.

■ ACKNOWLEDGMENTS

We thank Kyung Hwan Kim and Junbeom Jo for their help at the initial stage of the project. This work was supported by the Institute for Basic Science (IBS-R033). This work was supported by an internal R&D program at KAERI funded by the Ministry of Science and ICT (MIST) of the Republic of Korea (Grant 524420-23). This work was supported by a National Research Council of Science & Technology (NST) grant from the Korean Government (MSIT) (CAP-18-05-KAERI).

■ REFERENCES

(1) Davidsson, J.; Poulsen, J.; Cammarata, M.; Georgiou, P.; Wouts, R.; Katona, G.; Jacobson, F.; Plech, A.; Wulff, M.; Nyman, G.; Neutze, R. Structural determination of a transient isomer of CH_2I_2 by picosecond x-ray diffraction. *Phys. Rev. Lett.* **2005**, *94*, 245503.

(2) Ihee, H.; Lorenc, M.; Kim, T. K.; Kong, Q. Y.; Cammarata, M.; Lee, J. H.; Bratos, S.; Wulff, M. Ultrafast x-ray diffraction of transient molecular structures in solution. *Science* **2005**, *309*, 1223−1227.

(3) Cammarata, M.; Lorenc, M.; Kim, T. K.; Lee, J. H.; Kong, Q. Y.; Pontecorvo, E.; Lo Russo, M.; Schiró, G.; Cupane, A.; Wulff, M.; Ihee, H. Impulsive solvent heating probed by picosecond x-ray diffraction. *J. Chem. Phys.* **2006**, *124*, 124504.

(4) Kong, Q.; Wulff, M.; Lee, J. H.; Bratos, S.; Ihee, H. Photochemical reaction pathways of carbon tetrabromide in solution probed by picosecond x-ray diffraction. *J. Am. Chem. Soc.* **2007**, *129*, 13584−13591.

(5) Lee, J. H.; Kim, J.; Cammarata, M.; Kong, Q.; Kim, K. H.; Choi, J.; Kim, T. K.; Wulff, M.; Ihee, H. Transient x-ray diffraction reveals global and major reaction pathways for the photolysis of iodoform in solution. *Angew. Chem., Int. Ed.* **2008**, *47*, 1047−1050.

(6) Lee, J. H.; Kim, T. K.; Kim, J.; Kong, Q.; Cammarata, M.; Lorenc, M.; Wulff, M.; Ihee, H. Capturing transient structures in the elimination reaction of haloalkane in solution by transient x-ray diffraction. *J. Am. Chem. Soc.* **2008**, *130*, 5834−5835.

(7) Christensen, M.; Haldrup, K.; Bechgaard, K.; Feidenhans'l, R.; Kong, Q.; Cammarata, M.; Russo, M. L.; Wulff, M.; Harrit, N.; Nielsen, M. M. Time-resolved x-ray scattering of an electronically excited state in solution. Structure of the $^3A_{2u}$ State of tetrakis-μ-pyrophosphitodiplatinate(II). *J. Am. Chem. Soc.* **2009**, *131*, 502−508.

(8) Ihee, H. Visualizing solution-phase reaction dynamics with time-resolved x-ray liquidography. *Acc. Chem. Res.* **2009**, *42*, 356−366.

(9) Vincent, J.; Andersson, M.; Eklund, M.; Wöhri, A. B.; Odelius, M.; Malmerberg, E.; Kong, Q.; Wulff, M.; Neutze, R.; Davidsson, J. Solvent dependent structural perturbations of chemical reaction intermediates visualized by time-resolved x-ray diffraction. *J. Chem. Phys.* **2009**, *130*, 154502.

(10) Kim, T. K.; Lee, J. H.; Wulff, M.; Kong, Q.; Ihee, H. Spatiotemporal kinetics in solution studied by time-resolved x-ray liquidography (solution scattering). *ChemPhysChem* **2009**, *10*, 1958−1980.

(11) Haldrup, K.; Christensen, M.; Meedom Nielsen, M. Analysis of time-resolved x-ray scattering data from solution-state systems. *Acta Cryst. A* **2010**, *66*, 261−269.
(12) Ihee, H.; Wulff, M.; Kim, J.; Adachi, S. Ultrafast x-ray scattering: Structural dynamics from diatomic to protein molecules. *Int. Rev. Phys. Chem.* **2010**, *29*, 453−520.
(13) Jun, S.; Lee, J. H.; Kim, J.; Kim, J.; Kim, K. H.; Kong, Q.; Kim, T. K.; Lo Russo, M.; Wulff, M.; Ihee, H. Photochemistry of $HgBr_2$ in methanol investigated using time-resolved X-ray liquidography. *Phys. Chem. Chem. Phys.* **2010**, *12*, 11536−11547.
(14) Kim, J.; Lee, J. H.; Kim, J.; Jun, S.; Kim, K. H.; Kim, T. W.; Wulff, M.; Ihee, H. Structural dynamics of 1,2-diiodoethane in cyclohexane probed by picosecond x-ray liquidography. *J. Phys. Chem. A* **2012**, *116*, 2713−2722.
(15) Kim, K. H.; Muniyappan, S.; Oang, K. Y.; Kim, J. G.; Nozawa, S.; Sato, T.; Koshihara, S.; Henning, R.; Kosheleva, I.; Ki, H.; Kim, Y.; Kim, T. W.; Kim, J.; Adachi, S.; Ihee, H. Direct observation of cooperative protein structural dynamics of homodimeric hemoglobin from 100 ps to 10 ms with pump−probe x-ray solution scattering. *J. Am. Chem. Soc.* **2012**, *134*, 7001−7008.
(16) Neutze, R.; Moffat, K. Time-resolved structural studies at synchrotrons and x-ray free electron lasers: Opportunities and challenges. *Curr. Opin. Struct. Biol.* **2012**, *22*, 651−659.
(17) Lee, J. H.; Wulff, M.; Bratos, S.; Petersen, J.; Guerin, L.; Leicknam, J.-C.; Cammarata, M.; Kong, Q.; Kim, J.; Møller, K. B.; Ihee, H. Filming the birth of molecules and accompanying solvent rearrangement. *J. Am. Chem. Soc.* **2013**, *135*, 3255−3261.
(18) Kim, K. H.; Lee, J. H.; Kim, J.; Nozawa, S.; Sato, T.; Tomita, A.; Ichiyanagi, K.; Ki, H.; Kim, J.; Adachi, S.; Ihee, H. Solvent-dependent molecular structure of ionic species directly measured by ultrafast x-ray solution scattering. *Phys. Rev. Lett.* **2013**, *110*, 165505.
(19) Kim, K. H.; Ki, H.; Oang, K. Y.; Nozawa, S.; Sato, T.; Kim, J.; Kim, T. K.; Kim, J.; Adachi, S.; Ihee, H. Global reaction pathways in the photodissociation of I_3^- ions in solution at 267 and 400 nm studied by picosecond x-ray liquidography. *ChemPhysChem* **2013**, *14*, 3687−3697.
(20) Oang, K. Y.; Kim, J. G.; Yang, C.; Kim, T. W.; Kim, Y.; Kim, K. H.; Kim, J.; Ihee, H. Conformational substates of myoglobin intermediate resolved by picosecond x-ray solution scattering. *J. Phys. Chem. Lett.* **2014**, *5*, 804−808.
(21) Kim, K. H.; Kim, J. G.; Nozawa, S.; Sato, T.; Oang, K. Y.; Kim, T. W.; Ki, H.; Jo, J.; Park, S.; Song, C.; Sato, T.; Ogawa, K.; Togashi, T.; Tono, K.; Yabashi, M.; Ishikawa, T.; Kim, J.; Ryoo, R.; Kim, J.; Ihee, H.; Adachi, S. Direct observation of bond formation in solution with femtosecond x-ray scattering. *Nature* **2015**, *518*, 385−389.
(22) Kim, K. H.; Kim, J.; Oang, K. Y.; Lee, J. H.; Grolimund, D.; Milne, C. J.; Penfold, T. J.; Johnson, S. L.; Galler, A.; Kim, T. W.; Kim, J. G.; Suh, D.; Moon, J.; Kim, J.; Hong, K.; Guérin, L.; Kim, T. K.; Wulff, M.; Bressler, C.; Ihee, H. Identifying the major intermediate species by combining time-resolved x-ray solution scattering and x-ray absorption spectroscopy. *Phys. Chem. Chem. Phys.* **2015**, *17*, 23298−23302.
(23) Kim, J. G.; Kim, K. H.; Oang, K. Y.; Kim, T. W.; Ki, H.; Jo, J.; Kim, J.; Sato, T.; Nozawa, S.; Adachi, S.; Ihee, H. Rotational dephasing of a gold complex probed by anisotropic femtosecond x-ray solution scattering using an x-ray free-electron laser. *J. Phys. B: At. Mol. Opt. Phys.* **2015**, *48*, 244005.
(24) Kim, K. H.; Kim, J. G.; Oang, K. Y.; Kim, T. W.; Ki, H.; Jo, J.; Kim, J.; Sato, T.; Nozawa, S.; Adachi, S.; Ihee, H. Femtosecond x-ray solution scattering reveals that bond formation mechanism of a gold trimer complex is independent of excitation wavelength. *Struct. Dyn.* **2016**, *3*, 043209.
(25) Kim, J. G.; Muniyappan, S.; Oang, K. Y.; Kim, T. W.; Yang, C.; Kim, K. H.; Kim, J.; Ihee, H. Cooperative protein structural dynamics of homodimeric hemoglobin linked to water cluster at subunit interface revealed by time-resolved x-ray solution scattering. *Struct. Dyn.* **2016**, *3*, 023610.
(26) Haldrup, K.; Dohn, A. O.; Shelby, M. L.; Mara, M. W.; Stickrath, A. B.; Harpham, M. R.; Huang, J.; Zhang, X.; Møller, K. B.; Chakraborty, A.; Castellano, F. N.; Tiede, D. M.; Chen, L. X. Butterfly deformation modes in a photoexcited pyrazolate-bridged Pt complex measured by time-resolved x-ray scattering in solution. *J. Phys. Chem. A* **2016**, *120*, 7475−7483.
(27) Ki, H.; Oang, K. Y.; Kim, J.; Ihee, H. Ultrafast x-ray crystallography and liquidography. *Annu. Rev. Phys. Chem.* **2017**, *68*, 473−497.
(28) Oang, K. Y.; Yang, C.; Muniyappan, S.; Kim, J.; Ihee, H. SVD-aided pseudo principal-component analysis: A new method to speed up and improve determination of the optimum kinetic model from time-resolved data. *Struct. Dyn.* **2017**, *4*, 044013.
(29) Ahn, C. W.; Ki, H.; Kim, J.; Kim, J.; Park, S.; Lee, Y.; Kim, K. H.; Kong, Q.; Moon, J.; Pedersen, M. N.; Wulff, M.; Ihee, H. Direct observation of a transiently formed isomer during iodoform photolysis in solution by time-resolved x-ray liquidography. *J. Phys. Chem. Lett.* **2018**, *9*, 647−653.
(30) Marcellini, M.; Nasedkin, A.; Zietz, B.; Petersson, J.; Vincent, J.; Palazzetti, F.; Malmerberg, E.; Kong, Q.; Wulff, M.; van der Spoel, D.; Neutze, R.; Davidsson, J. Transient isomers in the photodissociation of bromoiodomethane. *J. Chem. Phys.* **2018**, *148*, 134307.
(31) Park, S.; Choi, J.; Ki, H.; Kim, K. H.; Oang, K. Y.; Roh, H.; Kim, J.; Nozawa, S.; Sato, T.; Adachi, S.; Kim, J.; Ihee, H. Fate of transient isomer of CH_2I_2: Mechanism and origin of ionic photoproducts formation unveiled by time-resolved x-ray liquidography. *J. Chem. Phys.* **2019**, *150*, 224201.
(32) Kim, J. G.; Nozawa, S.; Kim, H.; Choi, E. H.; Sato, T.; Kim, T. W.; Kim, K. H.; Ki, H.; Kim, J.; Choi, M.; Lee, Y.; Heo, J.; Oang, K. Y.; Ichiyanagi, K.; Fukaya, R.; Lee, J. H.; Park, J.; Eom, I.; Chun, S. H.; Kim, S.; Kim, M.; Katayama, T.; Togashi, T.; Owada, S.; Yabashi, M.; Lee, S. J.; Lee, S.; Ahn, C. W.; Ahn, D.-S.; Moon, J.; Choi, S.; Kim, J.; Joo, T.; Kim, J.; Adachi, S.; Ihee, H. Mapping the emergence of molecular vibrations mediating bond formation. *Nature* **2020**, *582*, 520−524.
(33) Park, C.-H.; Givens, R. S. New photoactivated protecting groups. 6. *p*-hydroxyphenacyl: A phototrigger for chemical and biochemical probes. *J. Am. Chem. Soc.* **1997**, *119*, 2453−2463.
(34) Conrad, P. G.; Givens, R. S.; Hellrung, B.; Rajesh, C. S.; Ramseier, M.; Wirz, J. *p*-hydroxyphenacyl phototriggers: The reactive excited state of phosphate photorelease. *J. Am. Chem. Soc.* **2000**, *122*, 9346−9347.
(35) Pelliccioli, A. P.; Wirz, J. Photoremovable protecting groups: Reaction mechanisms and applications. *Photochem. Photobiol. Sci.* **2002**, *1*, 441−458.
(36) Ma, C.; Chan, W. S.; Kwok, W. M.; Zuo, P.; Phillips, D. L. Time-resolved resonance Raman study of the triplet state of the *p*-hydroxyphenacyl acetate model phototrigger compound. *J. Phys. Chem. B* **2004**, *108*, 9264−9276.
(37) Ma, C.; Zuo, P.; Kwok, W. M.; Chan, W. S.; Kan, J. T. W.; Toy, P. H.; Phillips, D. L. Time-resolved resonance Raman study of the triplet states of *p*-hydroxyacetophenone and the *p*-hydroxyphenacyl diethyl phosphate phototrigger compound. *J. Org. Chem.* **2004**, *69*, 6641−6657.
(38) Ma, C.; Kwok, W. M.; Chan, W. S.; Zuo, P.; Wai Kan, J. T.; Toy, P. H.; Phillips, D. L. Ultrafast time-resolved study of photophysical processes involved in the photodeprotection of *p*-hydroxyphenacyl caged phototrigger compounds. *J. Am. Chem. Soc.* **2005**, *127*, 1463−1472.
(39) Zuo, P.; Ma, C.; Kwok, W. M.; Chan, W. S.; Phillips, D. L. Time-resolved resonance Raman and density functional theory study of the deprotonation reaction of the triplet state of *p*-hydroxyacetophenone in water solution. *J. Org. Chem.* **2005**, *70*, 8661−8675.
(40) Ma, C.; Kwok, W. M.; Chan, W. S.; Du, Y.; Kan, J. T. W.; Toy, P. H.; Phillips, D. L. Ultrafast time-resolved transient absorption and resonance Raman spectroscopy study of the photodeprotection and rearrangement reactions of *p*-hydroxyphenacyl caged phosphates. *J. Am. Chem. Soc.* **2006**, *128*, 2558−2570.
(41) Chen, X.; Ma, C.; Kwok, W. M.; Guan, X.; Du, Y.; Phillips, D. L. A Theoretical investigation of *p*-hydroxyphenacyl caged phototrigger compounds: An examination of the excited state photo-

https://doi.org/10.1021/acs.jpclett.3c00041
J. Phys. Chem. Lett. 2023, 14, 3103−3110

chemistry of *p*-hydroxyphenacyl acetate. *J. Phys. Chem. A* **2006**, *110*, 12406−12413.
(42) Chen, X.; Ma, C.; Kwok, W. M.; Guan, X.; Du, Y.; Phillips, D. L. A Theoretical investigation of *p*-hydroxyphenacyl caged phototrigger compounds: How water induces the photodeprotection and subsequent rearrangement reactions. *J. Phys. Chem. B* **2007**, *111*, 11832−11842.
(43) Givens, R. S.; Heger, D.; Hellrung, B.; Kamdzhilov, Y.; Mac, M.; Conrad, P. G.; Cope, E.; Lee, J. I.; Mata-Segreda, J. F.; Schowen, R. L.; Wirz, J. The photo-Favorskii reaction of *p*-hydroxyphenacyl compounds is initiated by water-assisted, adiabatic extrusion of a triplet biradical. *J. Am. Chem. Soc.* **2008**, *130*, 3307−3309.
(44) Stensrud, K.; Noh, J.; Kandler, K.; Wirz, J.; Heger, D.; Givens, R. S. Competing pathways in the photo-Favorskii rearrangement and release of esters: Studies on fluorinated *p*-hydroxyphenacyl-caged GABA and glutamate phototriggers. *J. Org. Chem.* **2009**, *74*, 5219−5227.
(45) Ma, C.; Kwok, W. M.; Chan, W. S.; Du, Y.; Zuo, P.; Kan, J. T. W.; Toy, P. H.; Phillips, D. L. Time-resolved spectroscopy studies of the photodeprotection reactions of *p*-hydroxyphenacyl ester phototrigger compounds. *Curr. Sci.* **2009**, *97*, 202−209.
(46) Cao, Q.; Guan, X.; George, M. W.; Phillips, D. L.; Ma, C.; Kwok, W. M.; Li, M.; Du, Y.; Sun, X.-Z.; Xue, J. Ultrafast time-resolved transient infrared and resonance Raman spectroscopic study of the photo-deprotection and rearrangement reactions of *p*-hydroxyphenacyl caged phosphates. *Faraday Discuss.* **2010**, *145*, 171−183.
(47) Givens, R. S.; Stensrud, K.; Conrad, P. G.; Yousef, A. L.; Perera, C.; Senadheera, S. N.; Heger, D.; Wirz, J. *p*-hydroxyphenacyl photoremovable protecting groups — Robust photochemistry despite substituent diversity. *Can. J. Chem.* **2011**, *89*, 364−384.
(48) Givens, R. S.; Rubina, M.; Wirz, J. Applications of *p*-hydroxyphenacyl (*p*HP) and coumarin-4-ylmethyl photoremovable protecting groups. *Photochem. Photobiol. Sci.* **2012**, *11*, 472−488.
(49) Givens, R. S.; Rubina, M.; Stensrud, K. F. Stereochemically probing the photo-Favorskii rearrangement: A mechanistic investigation. *J. Org. Chem.* **2013**, *78*, 1709−1717.
(50) Klán, P.; Šolomek, T.; Bochet, C.; Blanc, A.; Givens, R. S.; Rubina, M.; Popik, V.; Kostikov, A. P.; Wirz, J. Photoremovable protecting groups in chemistry and biology: Reaction mechanisms and efficacy. *Chem. Rev.* **2013**, *113*, 119−191.
(51) Jagadesan, P.; Da Silva, J. P.; Givens, R. S.; Ramamurthy, V. Photorelease of incarcerated guests in aqueous solution with phenacyl esters as the trigger. *Org. Lett.* **2015**, *17*, 1276−1279.
(52) Slanina, T.; Šebej, P.; Heckel, A.; Givens, R. S.; Klán, P. Caged fluoride: Photochemistry and applications of 4-hydroxyphenacyl fluoride. *Org. Lett.* **2015**, *17*, 4814−4817.
(53) Barman, S.; Mukhopadhyay, S. K.; Biswas, S.; Nandi, S.; Gangopadhyay, M.; Dey, S.; Anoop, A.; Singh, N. D. P. A *p*-hydroxyphenacyl−benzothiazole−chlorambucil conjugate as a real-time-monitoring drug-delivery system assisted by excited-state intramolecular proton transfer. *Angew. Chem., Int. Ed.* **2016**, *55*, 4194−4198.
(54) Houk, A. L.; Givens, R. S.; Elles, C. G. Two-photon activation of *p*-hydroxyphenacyl phototriggers: Toward spatially controlled release of diethyl phosphate and ATP. *J. Phys. Chem. B* **2016**, *120*, 3178−3186.
(55) Refson, K. Moldy: A portable molecular dynamics simulation program for serial and parallel computers. *Comput. Phys. Commun.* **2000**, *126*, 310−329.
(56) Frisch, M. J.; Trucks, G. W.; Schlegel, H. B.; Scuseria, G. E.; Robb, M. A.; Cheeseman, J. R.; Scalmani, G.; Barone, V.; Petersson, G. A.; Nakatsuji, H.; Li, X.; Caricato, M.; Marenich, A. V.; Bloino, J.; Janesko, B. G.; Gomperts, R.; Mennucci, B.; Hratchian, H. P.; Ortiz, J. V.; Izmaylov, A. F.; Sonnenberg, J. L.; Williams-Young, D.; Ding, F.; Lipparini, F.; Egidi, F.; Goings, J.; Peng, B.; Petrone, A.; Henderson, T.; Ranasinghe, D.; Zakrzewski, V. G.; Gao, J.; Rega, N.; Zheng, G.; Liang, W.; Hada, M.; Ehara, M.; Toyota, K.; Fukuda, R.; Hasegawa, J.; Ishida, M.; Nakajima, T.; Honda, Y.; Kitao, O.; Nakai, H.; Vreven, T.; Throssell, K.; Montgomery, J. A., Jr.; Peralta, J. E.; Ogliaro, F.; Bearpark, M. J.; Heyd, J. J.; Brothers, E. N.; Kudin, K. N.; Staroverov, V. N.; Keith, T. A.; Kobayashi, R.; Normand, J.; Raghavachari, K.; Rendell, A. P.; Burant, J. C.; Iyengar, S. S.; Tomasi, J.; Cossi, M.; Millam, J. M.; Klene, M.; Adamo, C.; Cammi, R.; Ochterski, J. W.; Martin, R. L.; Morokuma, K.; Farkas, O.; Foresman, J. B.; Fox, D. J. *Gaussian 16*, revision C.01; Gaussian, Inc.: Wallingford, CT, 2016.
(57) Chen, J.; Brooks, C. L. Critical importance of length-scale dependence in implicit modeling of hydrophobic interactions. *J. Am. Chem. Soc.* **2007**, *129*, 2444−2445.
(58) Chen, J.; Brooks, C. L., III Implicit modeling of nonpolar solvation for simulating protein folding and conformational transitions. *Phys. Chem. Chem. Phys.* **2008**, *10*, 471−481.

https://doi.org/10.1021/acs.jpclett.3c00041
J. Phys. Chem. Lett. 2023, 14, 3103−3110